Expression and Regulation of S100 Fused-Type Protein Hornerin at the Ocular Surface and Lacrimal Apparatus

Fabian Garreis,[1] Janine Jahn,[1] Katharina Wild,[1] Daniel B. Abrar,[1] Martin Schicht,[1] Jens-Michael Schröder,[2] and Friedrich Paulsen[1]

[1]Department of Anatomy II, Friedrich Alexander University Erlangen-Nürnberg (FAU), Erlangen, Germany
[2]Department of Dermatology, University Hospital Schleswig-Holstein, Kiel, Germany

Correspondence: Fabian Garreis, Friedrich Alexander University Erlangen-Nürnberg (FAU), Department of Anatomy II, Universitätsstraße 19, 91054 Erlangen, Germany; fabian.garreis@fau.de.

Submitted: July 17, 2017
Accepted: October 12, 2017

Citation: Garreis F, Jahn J, Wild K, et al. Expression and regulation of S100 fused-type protein hornerin at the ocular surface and lacrimal apparatus. *Invest Ophthalmol Vis Sci*. 2017;58:5968–5977. DOI:10.1167/iovs.17-22637

Purpose. The S100 fused-type proteins hornerin (HRNR) and filaggrin-2 (FLG2) are members of the epidermal differentiation complex, which is involved in terminal differentiation of keratinocytes via cornification as well as maintenance of the epidermal antimicrobial barrier. We investigated the expression and possible regulation of HRNR and FLG2 at the ocular surface and in the lacrimal apparatus.

Methods. Tissues of the lacrimal apparatus and ocular surface were analyzed systematically by means of RT-PCR, immunohistochemistry, and immuntransmission electron microscopy (iTEM) for their ability to express and produce HRNR and FLG2. In addition, inducibility and regulation of HRNR were studied in cultivated human corneal (HCE), conjunctival (HCjE), as well as meibomian gland (HMGEC) epithelial cell line by real-time RT-PCR.

Results. RT-PCR, immunohistochemistry, and iTEM revealed constitutive expression of HRNR in the epithelium of cornea, conjunctiva, nasolacrimal ducts, and acinus cells of lacrimal and meibomian glands. HRNR also was detected in tears of healthy volunteers. No expression of FLG2 could be detected in tissue samples of the ocular surface and lacrimal apparatus. Real-time RT-PCR revealed a decreased *HRNR* gene expression after challenge with proinflammatory cytokines and supernatants of *Escherichia coli* and *Pseudomonas aeroginosa* in HCE cells, whereas HCjE cells revealed no changes. In HMGECs serum-induced differentiation and application of all-trans retinoic acid significantly increased *HRNR* gene expression.

Conclusions. The data suggest that HRNR, but not FLG2, is a component of the ocular surface and lacrimal apparatus, including meibomian glands. HRNR seems to contribute to the maintenance of the epithelial barrier at the ocular surface and, thus, also may be involved in ocular surface diseases.

Keywords: hornerin, HNRN, filaggrin-2, FLG2, S100 fused-type proteins, SFTPs, epidermal differentiation complex, EDC, lacrimal apparatus, ocular surface, meibomian gland dysfunction, MGD, dry eye disease, DED, antimicrobial peptides, AMPs

Corneal and conjunctival epithelial cells, together with tear film compounds and blinking, are an essential part of the ocular surface barrier against invading pathogens. The importance of visual perception and the exposed localization of the ocular surface are reasons for a highly diverse repertoire of antimicrobial compounds in tears. Well known "classical" tear antimicrobial components, such as lysozyme, lactoferrin, tear-lipocalin, secretory immunoglobulin A (sIgA), as well as compounds of the complement system, occur in milligram range in tears and show broad antimicrobial activity.[1] In addition, tears contain a great bulk of other compounds, many of them with antimicrobial activity. These components are present in a much lower concentration (pico- to microgram) in tears. Beside their antimicrobial activity, several of these compounds have other activities as main biological function and several have been detected with yet unknown function at the ocular surface.[2] In the last decade, several antimicrobial peptides (AMPs) have been isolated from human skin. Human keratinocytes express and released various skin-derived AMPs, such as human β-defensins (hBD), cathelicidin LL-37, S100 proteins, protease inhibitors, and members of the ribonuclease A family.[3,4] In previous studies, we showed functional expression of skin-derived AMPs, such as hBDs, as well as the S100 calcium-binding protein A7 (S100A7, psoriasin) in cells of the ocular surface, lacrimal apparatus, and tears.[5–7]

We analyzed expression and regulation of the S100 fused-type proteins (SFTPs) hornerin (HRNR), and filaggrin-2 (FLG2, ifapsoriasin) at the ocular surface and lacrimal apparatus. Both proteins are essential molecules of healthy epidermis that maintain epidermal homeostasis and barrier function.[8,9] The corresponding genes are located within the epidermal differentiation complex (EDC) on human chromosome 1q21.[10,11] The EDC includes three gene families: (1) late cornified envelope (LCE) precursors and small proline-rich proteins (SPRP), (2) calcium-binding S100A, and (3) S100 fused-type genes.[12] In human, SFTPs include profilaggrin, filaggrin, trichohyalin, repetin, cornulin, as well as HRNR and FLG2. All combine a similar gene structure and all share equal protein domains, that is, two EF-hand calcium-binding domains in the N-terminal region.[12]

Human HRNR was first described in wounded and psoriatic epidermis, but not in healthy skin.[13] Using biochemical

Table. Gene-Specific Oligonucleotide Primer for Real-time RT-PCR

Gene	Accession-Number	Sense Primer (5′-3′)	Antisense Primer (5′-3′)	UPL Probe
HRNR	NM_001009931.1	atgagtctgcctcccatcac	agactgccctgacccaga	#21
18S ribosomal RNA (reference gene)	X03205.1	ggtgcatggccgttctta	tgccagagtctcgttcgtta	#22

Primer design was performed by Universal ProbeLibrary (UPL) Assay Design Center from Roche.

analyses, HRNR protein fragments have been identified in stratum corneum of healthy skin and antibodies against repeat domains of HRNR also have localized HRNR expression in healthy human epidermis.[8] Here, HRNR is localized in the stratum granulosum and stratum corneum and forms high molecular weight multimeric HRNR fragment complexes. Moreover, HRNR contributes to the cornified envelope and HRNR fragments show antimicrobial and protective functions in healthy skin. The full-length HRNR protein is auto-processed by an unknown mechanism into multiple novel fragments with antimicrobial activity to gram-negative bacteria and fungi.[8,14] A reduction in HRNR expression is associated with epidermal barrier defects, which have been observed in patients with atopic dermatitis, a common chronic inflammatory skin disease.[8,15] Like HRNR, FLG2 also is localized in the stratum granulosum and corneum of human epidermis.[9] C-terminal fragments of FLG2 were potent antimicrobials, especially toward *Pseudomonas aeruginosa*, by interfering with the bacterial replication.[16] According to its amino acid composition, FLG2 can contribute to stratum corneum hydration ("natural moisturizing factor"), photoprotection as well as formation of the epidermal barrier.[9]

Only limited information is available with regard to the biological functions of most EDC members at the ocular surface. Various EDC members, including *Escherichia coli*-killing S100A7 and S100A8/A9 heterodimer calprotectin, have been shown to be involved in innate immune defense at the ocular surface.[6,17] Therefore, we clarified whether skin-derived, antimicrobially-active HRNR and FLG2 are expressed and contribute to epithelial immune defense at the ocular surface.

Material and Methods

Tissues, Tears, and Cell Lines

Tissues of the ocular surface and lacrimal apparatus were obtained from cadavers (aged 41–93 years) donated to the Department of Anatomy and Cell Biology, Martin Luther University Halle-Wittenberg, Germany. All subjects signed a testamentary permission in time. The study included proper consent and approval, complied with the tenets of the Declaration of Helsinki, and was approved by institutional review board regulations. The body donors were free of recent trauma, eye and nasal infections, and diseases involving or affecting lacrimal function. All tissues were dissected from cadavers within a time frame of 4 to 24 hours postmortem. After dissection, the tissues were prepared for paraffin-embedding by 4% paraformaldehyde (PFA) fixation or were used for molecular biological investigation and were frozen immediately at −80°C. Tears were obtained from healthy, noncontact lens wearers (three women, three men; 22–37 years) with Schirmer strips without anesthetics. Sampling and preparation was done as described previously.[18]

In addition, three cell lines were used:[19–21] a SV40-transformed human corneal epithelial (HCE) cell line (kindly provided by Kaoru Araki-Sasaki, Tane Memorial Eye Hospital, Osaka, Japan), an immortalized human conjunctival epithelial (HCjE) cell line (kindly provided by Ilene K. Gibson, Schepens Eye Research Institute, Harvard Medical School, Boston, MA, USA), and an immortalized human meibomian gland epithelial (HMGEC) cell line (kindly provided by David Sullivan, Schepens Eye Research Institute, Harvard Medical School).

Cell Culture

Immortalized HCE, HCjE, and HMGEC cells were cultured as reported previously[6,22,23] in a humidified incubator at 37°C under standard condition (21% O_2, 5% CO_2). For stimulation experiments, 5×10^6 cells were seeded in Petri dishes; at approximately 90% confluence cells were exposed to IL-1β (10 ng/mL; ImmunoTools, Friesoythe, Germany), TNF-α (10 ng/mL; ImmunoTools) or heat-inactivated supernatants of *Staphylococcus aureus*, *P. aeruginosa*, and *E. coli* (each 1:100 dilution). Furthermore, cells were cultivated under hypoxic conditions (5% O_2, 5% CO_2) or exposed to 30 mJ/cm^2 UV-B radiation in a radiation chamber. Afterwards cells subsequently were cultivated further under standard conditions. HMGEC cells cultivated in serum-free (SfM) as well as serum-containing (ScM) medium were cocultivated with 2 μM all-trans retinoic acid (ATRA; R1474; Spectrum Chemical, New Brunswick, NJ, USA). Cells with solvent alone or without radiation were cultivated at standard conditions (37°C, 21% O_2, 5% CO_2) and used as control. All experiments were performed for 24 hours.

RNA Isolation and RT-PCR

Total RNA was extracted from confluent cell cultures as well as human tissues using peqGOLD TriFast reagent (Peqlab, Germany). Tissue was crushed mechanically in 1 mL Trifast reagent in innuSPEED Lysis Tube by using SpeedMill plus (both Analytik Jena AG, Jena, Germany). After centrifugation (10 minutes, 15,520*g*) supernatants were used for RNA isolation. DNA contamination was eliminated by digestion with RNase-free DNase I (30 minutes at 37°C). The DNase was heat inactivated for 10 minutes at 65°C. Reverse transcription of RNA samples to first-strand cDNA was performed by RevertAid H Minus M-MuL V Reverse Transcriptase Kit (Fermentas, Darmstadt, Germany) according to manufacturer's protocol. Two micrograms total RNA and 10 pmol Oligo (dT) 18 primer (Fermentas) were used for each reaction. Each PCR reaction contained 2 μL cDNA in 2.5 μL 10x PCR buffer, 1 μL 50 mM $MgCl_2$, 1 μL 10 mM dNTP mix (Fermentas), 0.5 μL 10 pmol forward primer, 0.5 μL 10 pmol reverse primer, 0.2 μL (5 U/μL) Taq DNA Polymerase (Invitrogen, Darmstadt, Germany) contained in 25 μL RNase-free DEPC-treated water. HRNR PCR amplification underwent an initial cycle at 95°C for 5 minutes followed by 35 cycles at 95°C for 20 seconds, 60°C for 20 seconds, 72°C for 1 minute and a final elongation at 72°C for 3 minutes as well as a temperature hold at 4°C. Gen-specific intron-spanning primer sequences, annealing temperatures, cycle numbers, and product sizes are shown in the Table. Primers were synthesized at MWG Biotech AG (Ebersberg, Germany). PCR products were analyzed by electrophoresis in a 1.5% agarose gel and visualized via fluorescence. Base pair (bp) values were compared with Genbank data. Reactions without reverse transcriptase during cDNA synthesis were performed to rule out genomic DNA contamination. Reference gene β-

actin served as internal control for assessing integrity and stability of the transcribed cDNA.

Real Time RT-PCR

Real-time RT-PCR quantified *HRNR* gene expression. Each reaction was performed in a final volume of 20 µL containing 10 µL LightCycler 480 Probe Mastermix (Roche, Basel, Switzerland), 0.4 µL gene-specific UPL probe, 0.5 µL gene-specific primer mix (10 pmol; Table), 7.1 µL nuclease-free water, and 2 µL sample cDNA. Each plate was run at 95°C for 10 minutes, followed by 55 cycles of 95°C for 10 seconds, 60°C for 30 seconds, and 72°C for 1 second. The cycle threshold (Ct) parameter was defined by second derivative maximum analysis with LightCyler480 software v1.5. To standardize mRNA concentration transcript levels of a reference gene in each sample, 18S rRNA was determined in parallel and relative transcript levels were corrected by normalization with the 18S Ct levels. All real-time RT-PCRs were performed in triplicate and changes in gene expression were calculated using the delta delta Ct method. Real-time RT-PCR was performed using LightCycler 480 from Roche.

Western Blot

Cadaver tissues (~100 mg) were lysed in 300 µL 1% Triton X-100 with protease- and phosphatase inhibitor in an innuSPEED Lysis Tube A placed in a SpeedMill plus homogenizer (both Analytik Jena AG). Then, samples were centrifuged at 18,214*g* for 5 minutes and supernatants used for further analysis and stored at −80°C. Protein concentration of tissue extracts and tear samples were determined with the Bradford assay. For Western blot analysis, 20 µg total protein was boiled for 5 minutes with a reducing buffer containing β-mercaptoethanol and loaded onto 10% SDS polyacrylamide gel, separated by electrophoresis and transferred to a nitrocellulose membrane by blotting. Blots were blocked in 5% nonfat milk/PBST (1 mL Tween 20 /1 L 1x PBS) for 1 hour and probed overnight at 4°C with a goat polyclonal HRNR antibody mixture (1:1.000 dilution) against H2, H3, and H4 epitopes, described previously.[8] PBST washing was followed by incubation with horseradish peroxidase conjugated secondary antibody (1:5.000 dilution, 2 hours at room temperature [RT]). Signal readout was determined by chemiluminescence with an ECL substrate (Millipore, Darmstadt, Germany) in Biorad Universalhood II.

Immunohistochemistry

Human tissue obtained from cadavers was fixed in 4% paraformaldehyde, embedded in paraffin, sectioned (7 µm), and then deparaffinized. Immunohistochemical staining was performed as described previously.[7] Visualization was achieved with horseradish peroxidase-labeled streptavidin-biotin complex (StreptABComplex/HRP; Dako, Santa Clara, CA, USA) and 3,3′-diaminobenzidine (DAB; Dako). Sections were counterstained with hemalum and mounted in Entellan (Dako). Not commercially available goat polyclonal antibodies against HRNR and FLG2 were used in a final concentration of 0.01 mg/mL. All primary antibodies were generated and validated by the group of J. M. Schröder. Antibodies were affinity purified and specificity was tested by immuno-dot analyses and Western blots using purified HRNR and FLG-2 peptides. All antibodies were free of cross-reactivity.[8,9] Furthermore, control sections were incubated with nonimmune IgG to determine possible nonspecific binding of IgG. All slides were examined with a Keyence BZ 9000 microscope.

Immuno-Transmission Electron Microscopy (iTEM)

Three lower eyelids, including mucocutaneous junction (MCJ) and meibomian gland orifice, from three body donors were used for iTEM analysis. Lids were prepared and fixed in 4% PFA in PBS for 4 hours at 4°C. The fixed tissue samples then were immersed in 1 M sucrose in PBS for at least 24 hours and subsequently were frozen in liquid nitrogen. For pre-embedding immunocytochemistry, 25-µm cryostat sections were cut and mounted on coverslips (Thermanox; Nunc, Rochester, NY, USA). Cryosections were blocked in 1% low-fat milk powder, 0.001% Tween 20 and PBS for 30 minutes at room temperature. The anti-HRNR antibody (H4 epitope) was applied in 2% BSA/PBS and incubated overnight at 4°C. After five rinses with 0.5% BSA/PBS, the sections were incubated overnight at 4°C with ultrasmall gold-conjugated anti-mouse F(ab′)2 (Roth, Karlsruhe, Germany) in 0.5% BSA/PBS. Sections then were rinsed five times with 0.5% BSA/PBS and two times with PBS and were fixed with 2.5% glutaraldehyde in PBS for 1 hour at 4°C. Afterwards silver enhancement was performed (R-Gent SE-EM; Aurion, Wageningen Netherlands) for 35 minutes in darkness. Sections were postfixed with 1% osmium tetroxide (OsO_4) in PBS for 30 minutes and embedded in Epon (Roth). Ultrathin sections (50 nm) of the specimens were cut, contrasted with uranyl acetate for 5 minutes, washed, and air dried. All slides were examined in a transmission electron microscope (JEOL TEM-1400 Plus, Freising, Germany). Apart from the omission of the primary antibody, the control sections were treated the same way. No control section showed labeling with gold particles.

Statistics

Results are plotted as means ± SEM. Gaussian distribution was determined by the Kolmogorov–Smirnov test. After evaluating values for normal distribution, we performed 1-way ANOVA statistics. For interpretation of the results, we used either Bonferroni or Dunn post hoc tests. All bar charts were generated and analyzed with GraphPad Prism (version 5). *P* values less than 0.05 were considered statistically significant.

Results

HRNR Gene Expression in the Lacrimal Apparatus

HRNR, but not *FLG2*, transcripts were detected in tissue samples of the ocular surface and lacrimal apparatus obtained from body donors (Fig. 1A). RT-PCR analysis showed *HRNR* transcripts in all four analyzed corneal samples, four of five conjunctival samples, nine of 10 lacrimal gland samples, and six of nine nasolacrimal duct samples. Furthermore, *HRNR* transcripts were present in HCE and HCjE cells. *FLG2* transcript was detected only in two of nine nasolacrimal duct samples. All other tissue samples as well as cell lines that were examined for *FLG2* revealed no gene expression (data not shown). Human skin (cutis) was used as positive control (PC) and, as expected, revealed a signal for *HRNR* and *FLG2*. The β-actin control PCR products were invariant in all samples. In the no template control (Ø) obtained by omitting the reverse transcription through cDNA synthesis, no transcript was detected. This negative result confirmed specific amplification of cDNA and the absence of contaminating genomic DNA. Western blot analysis (Fig. 1B) revealed HRNR protein expression in human tears obtained from healthy donors ($n = 6$). Interestingly, Western blot analysis with a mixture of antibodies toward various HRNR epitopes (H2, -3, and -4) showed specific bands at approximately 100, 70, 50, and 25 kDa in tears. In contrast, tissue extracts from lacrimal gland

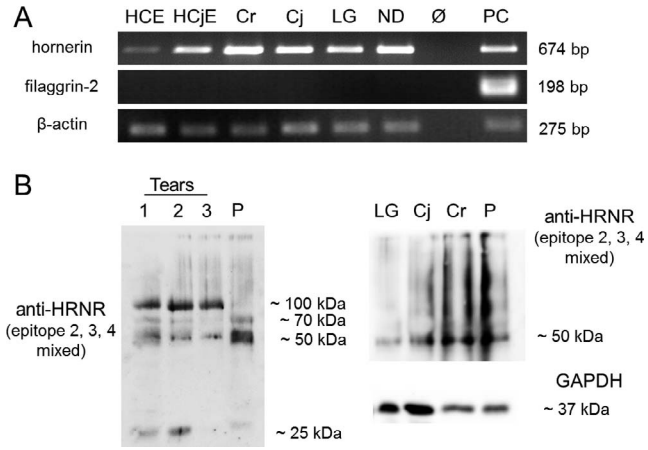

Figure 1. HRNR and FLG2 expression in cells and tissues of the lacrimal apparatus. (**A**) RT-PCR analysis reveals gene expression of HRNR in immortalized HCE and HCjE cells, Cr, Cj, LG, and nasolacrimal duct (ND). FLG2 transcript was not detectable. Blot represents results from tissues obtained from different cadavers ($n = 4$–10). β-actin RT-PCR was performed as a control of cDNA quantity. Controls without *RT* step in cDNA synthesis (ø) and with cDNA from human skin (PC) were used. (**B**) HRNR protein expression in tears from three healthy donors (1-3) and tissue extracts from LG, Cj, Cr, and skin (P). Western blot analysis of tissue extracts with a mixture of antibodies toward HRNR2, HRNR3, and HRNR4. Representative results of three independent Western blot analyses are shown.

(LG), conjunctiva (Cj), and cornea (Cr) obtained from cadavers ($n = 3$) showed only a specific band at 50 kDa. Controls obtained from human skin (cutis) also demonstrated a clear band at 50 kDa, and a much weaker band at 70 kDa with HRNR antibodies mixture.

Immunolocalization of HRNR in the Lacrimal Apparatus

To localize HRNR protein at the ocular surface and lacrimal apparatus, immunohistochemical analysis of formalin-fixed paraffin-embedded tissue sections (7 μm) from cadavers was performed. The distribution of HRNR in the tissues was as follows:

Cornea. All analyzed corneae (10/10) showed HRNR immunoreactivity in all epithelial as well as endothelial cells but not in corneal stromal fibroblasts (Fig. 2A).

Conjunctiva. All conjunctivae (10/10) revealed HRNR antibody reactivity. HRNR was visible intracytoplasmically in high columnar epithelial cells as well as basal cells of the conjunctiva (Fig. 2B). The secretory product of goblet cells and goblet cells alone demonstrated no reactivity.

Nasolacrimal Ducts. HRNR immunoreactivity was visible in seven of 10 different samples from cadavers. Immunoreactivity occurred intracytoplasmically in high columnar epithelial cells and in basal cells of the epithelial layer, but not in goblet cells. Stronger immunoreactivity was visible at the apical surface of nasolacrimal duct epithelial cells (Fig. 2D).

Lacrimal Gland. Six of 10 samples showed weak intracytoplasmatic HRNR antibody reactivity in the acinus cells (Fig. 2E). Four of the six positive cases revealed clear regional difference in the HRNR distribution.

Eyelid and Eyelid-Glands. In all analyzed eyelids (10/10) an intensive HRNR immunoreactivity was detected in the epidermis, hair follicles of the eyelashes, as well as eyelid-associated glands (Figs. 2C, 3). All keratinocytes in the epidermis showed HRNR antibody reactivity in all layers. A weak reactivity was visible in keratinocytes of the stratum basale, whereas keratinocytes in the stratum spinosum, stratum granulosum, and stratum corneum showed stronger reactivity. Also, strong immunoreactivity was visible in epithelial cells of hair follicles. The epidermis layer and hair follicle layer indicated an increasing intensity from basal to apical. Acinar cells of the hair-associated sebaceous glands (glands of Zeis) as well as modified apocrine sweat glands (glands of Moll) showed HRNR antibody reactivity. Further, immunoreactivity of meibomian glands was observed. HRNR antibody reactivity was present in meibocytes (acinar cells) and in epithelial cells of the excretory ducts of the meibomian glands (Fig. 3).

FLG2 immunoreactivity could not be detected in tissue sections of the ocular surface and lacrimal apparatus from cadavers. Only the apical layer of the epidermis and hair follicles in the eyelids revealed a clear FLG2 antibody reactivity. In addition, immunoreactivity was visible in vascular endothelial cells in the lamina propria (Supplementary Fig. S1). Immunohistochemistry with nonimmune IgG instead of the HRNR or FLG2 antibodies showed no immunoreactivity for each investigated tissue (Fig. 2F).

iTEM analysis was performed to examine more precisely the subcellular localization of HRNR in the epithelium of the central duct near the meibomian gland orifice (MGO). Results indicated a clear HRNR accumulation in para-keratinized epithelial cells of the central excretory duct of meibomian glands. Here, HRNR accumulates in an amorphous material of moderate electron-density (Figs. 4A, 4B). In the epidermis of human eyelid HRNR specific antibodies are partly localized in keratinocytes of the stratum granulosum and enhance gold particle enrichment in keratinocytes of the stratum corneum. Higher magnifications clearly show HRNR accumulation occurs in filamentous structures of moderate electron-density. Immunogold-labeled HRNR antibodies are associated with amyloid-like nanostructures (Figs. 4C, 4D).

Regulation of *HRNR* Gene Expression in HCE and HCjE Cells

To investigate the regulation of HRNR under conditions mimicking clinical symptoms of dry eye disease (DED, keratoconjunctivitis sicca) as well as bacterial infection at the ocular surface (keratitis, blepharitis) we analyzed *HRNR* gene expression in immortalized HCE and HCjE cells that were treated with proinflammatory cytokines as well as supernatants of *S. aureus*, *P. aeruginosa*, and *E. coli*. Furthermore, we analyzed stress-induced HRNR expression after UV-B exposure and cultivation by hypoxic conditions.

In HCE cells quantitative real-time RT-PCR revealed significant downregulation of *HRNR* transcript after treatment with IL-1β (0.4 ± 0.20-fold; $P < 0.05$) and TNF-α (0.3 ± 0.12-fold; $P < 0.05$) compared to controls (1.0 ± 0.20; Fig. 5A). Supernatants of *S. aureus* (8.2 ± 2.85-fold, $P < 0.05$) increased *HRNR* gene expression, whereas supernatants of *P. aeruginosa* (1.3 ± 0.31-fold) and *E. coli* (0.5 ± 0.08-fold) did not show any significant effect with regard to the *HRNR* gene expression (Fig. 5B). Cultivation under hypoxic conditions ($P_{O2} = 5\%$) increased the *HRHN* gene expression (8.8 ± 2.98-fold, $P = 0.0249$) whereas UV-B exposure (1.6 ± 0.72-fold) had no effect compared to controls. Also increased Ca^{2+} concentrations did not influence *HRNR* gene expression after 24 hours in cultivated HCE cells (Fig. 5D).

In HCjE cells, only hypoxic conditions significantly affected the *HRNR* gene expression compared to untreated cells. Cultivation of HCjE cells under decreased oxygen partial pressure led to induction of *HRNR* gene expression up to 1.8 ± 0.31-fold ($P = 0.0262$) compared to standard cultivation by $P_{O2} = 21\%$ (1.0 ± 0.14; Fig. 5C). In contrast, treatment with IL-β (0.7 ± 0.09-fold), TNF-α (1.1 ± 0.20-fold), supernatants of *S.*

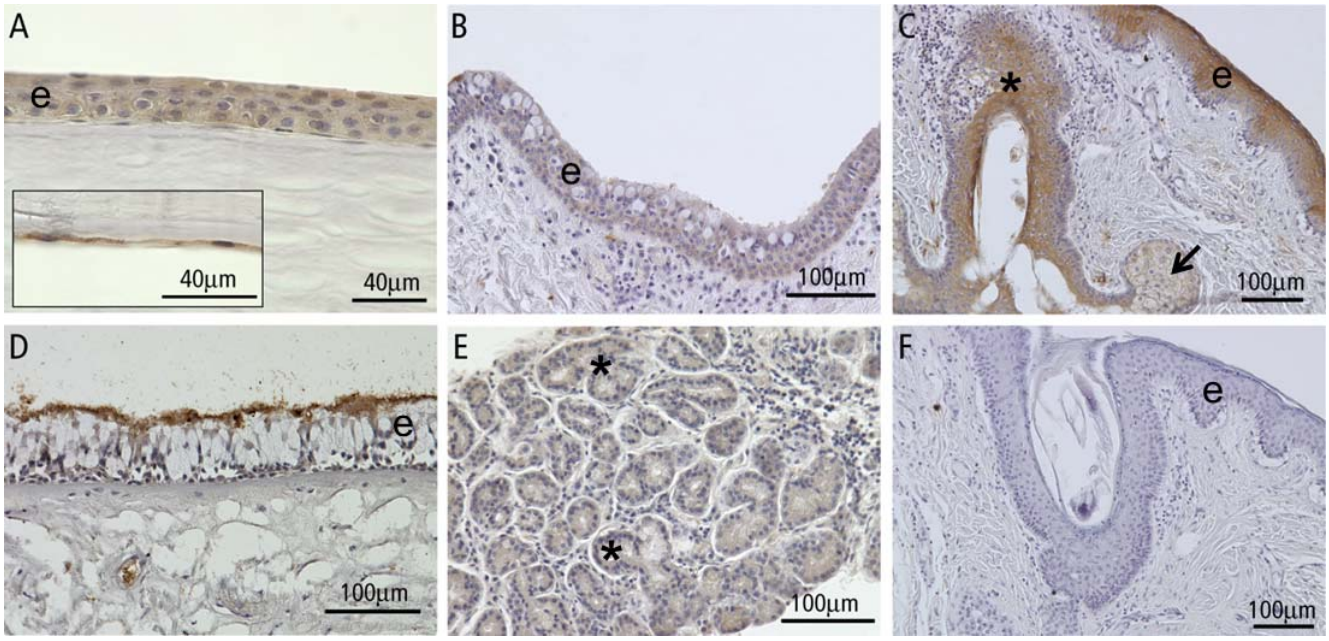

Figure 2. Immunohistochemical analysis of HRNR expression at the ocular surface and in the lacrimal apparatus. Localization of HRHR is marked by immunoreaction (*brown*) in epithelial cells (e) of the cornea (**A**), conjunctiva (**B**), epidermis, and hair follicle (*) of the eyelid (**C**), nasolacrimal duct (**D**) and in acinar cells (*) of the lacrimal gland (**E**). Immunohistochemistry with nonimmune IgG instead of the HRNR antibody shows no immunoreactivity (**F**). Pictures represent meaningful immunohistochemical analyses of 10 different cadaver samples. Nuclei are counterstained with hemalum (*blue*).

aureus (1.6 ± 0.62-fold), *P. aeruginosa* (1.6 ± 0.33-fold), or *E. coli* (0.9 ± 0.13-fold) as well as UV-B exposure (1.6 ± 0.72-fold) did not regulate the *HRNR* gene expression in HCjE cells compared to controls. Increased Ca^{2+} concentrations also had no effect on the *HRNR* gene expression after 24 hours in cultivated HCjE cells.

HRNR in HMGECs

Immunohistochemical analysis revealed a strong HRNR signal in epithelial cells of the excretory ducts as well as meibocytes (acinar cells) of the meibomian glands from human cadavers (Fig. 3). Our RT-PCR experiments showed *HRNR* gene

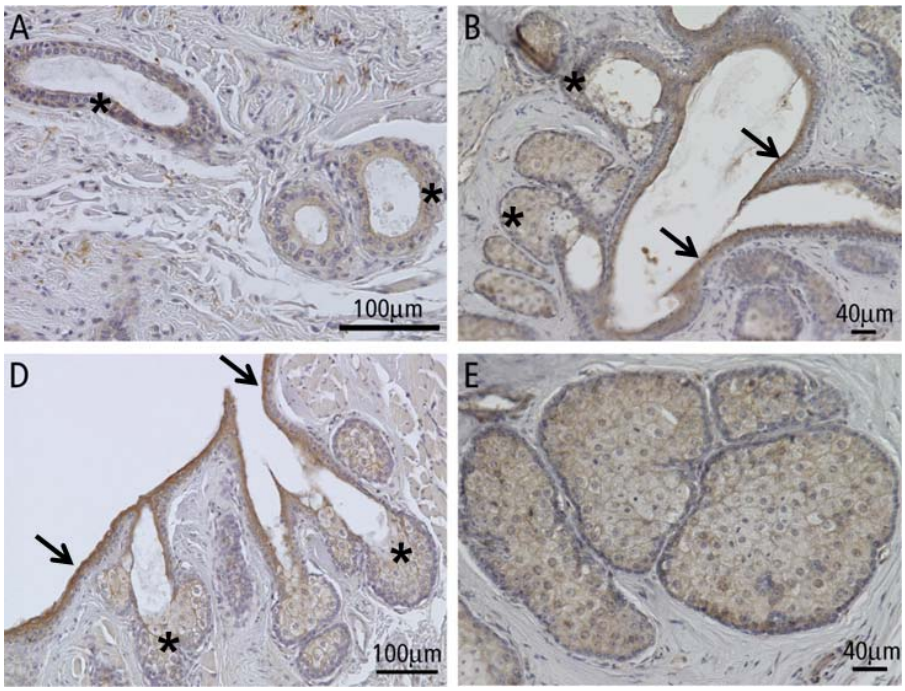

Figure 3. Immunohistochemical analysis of HRNR expression in the human meibomian gland. HRHR immunoreactivity is visible in epithelial cells (*) of glands of Moll (**A**), in meibocytes (*) and in epithelial cells (*arrows*) of the excretory duct of the meibomian gland (**B–E**). Pictures represent meaningful immunohistochemical analyses of 10 different cadaver samples. Nuclei are counterstained with hemalum (*blue*).

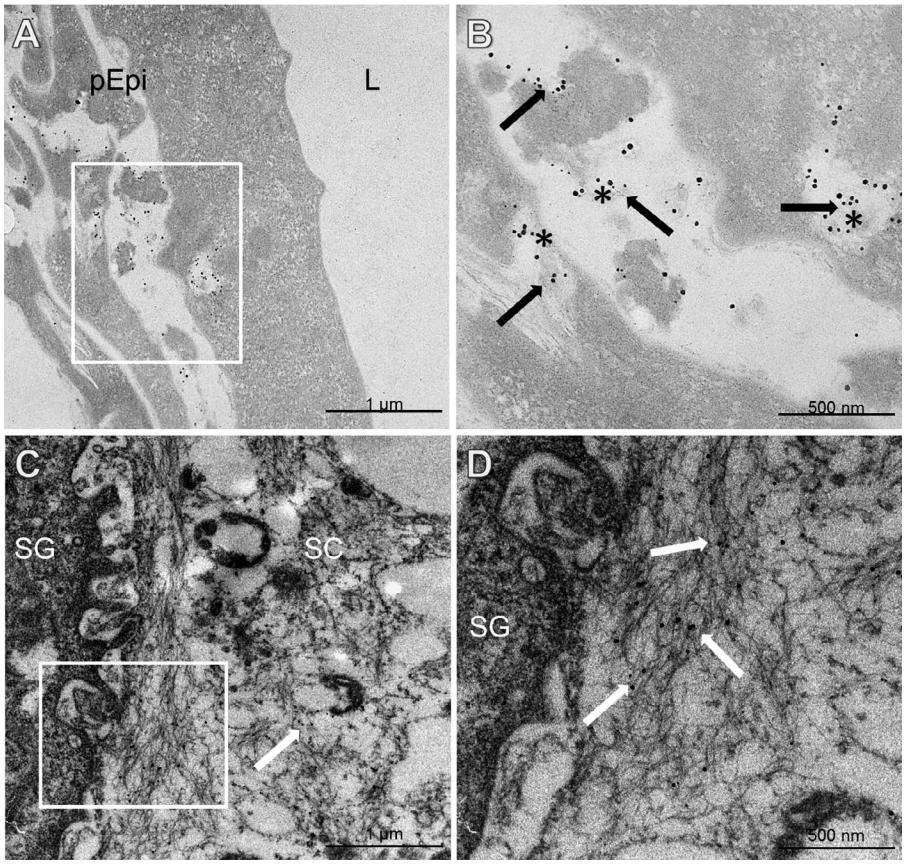

Figure 4. Localization of HRNR by iTEM in human eyelid. (**A**) HRNR localization in para-keratinized epithelium (pEpi) of the central excretory duct of a human meibomian gland. (**B**) Inlet in higher magnification. Gold particles (*arrows*) corresponding to HRNR and show accumulation to electron dense amyloid-like (*) nanostructures. (**C**) HRNR localization in human eyelid epidermis. (**D**) Inlet in higher magnification. Immunogold-labeled antibodies to HRNR (*arrows*) accumulate on filament-like structures in the stratum corneum (SC). The pictures show representative results of three independent samples. Magnification: (**A**, **C**) 12,000-fold, (**B**, **D**) 30,000-fold, Stratum granulosum (SG), duct lumen (L).

expression in immortalized human meibomian gland epithelial cells (cell line HMGEC) cultivated in serum-free (SfM) and serum-containing medium (ScM) (Fig. 6A). Furthermore, the used HRNR antibody showed intracytoplasmic immunoreactivity in serum-differentiated HMGECs (Fig. 6B). Real-time RT-PCR demonstrated a significant increase of the *HRNR* gene expression in serum-differentiated HMGECs (5.6 ± 0.89) compared to serum-free cultivated HMGECs (1.1 ± 0.20, $P = 0.0022$) (Fig. 6C). ATRA is well-known to influence meibocyte physiology.[24] Our real-time RT-PCR results demonstrated that treatment with 2 µM ATRA had a significant effect on the gene expression of HRNR in immortalized HMGEC cultivate in SfM. Treatment with ATRA enhanced the *HRNR* gene expression up to 3.6 ± 0.63-fold ($P = 0.0016$) compared to untreated cells (1.2 ± 0.19). In contrast, ATRA had no effect on *HRNR* gene expression in HMGECs cultivated in serum-containing medium (Fig. 6D).

Discussion

Our study demonstrated expression of SFTP HRNR in various cells of the ocular surface, lacrimal apparatus, and in tears, whereas in contrast FLG2 (ifapsoriasin) expression is absent (Figs. 1–3). Our HRNR expression results in the epidermis of the eyelids and skin-associated hair follicles are consistent with the expression pattern in various skin areas from human biopsies.[8] Remarkably, our analyses demonstrated immunoreactivity in the lipid-producing, holocrine meibocytes as well as in epithelial cells of the excretory ducts of meibomian glands (Fig. 3). Our ultrastructural analysis verifies these results and demonstrates clear HRNR accumulation in the (para) keratinized epithelium of the terminal part of the central duct close to the meibomian gland orifice and to keratinocytes of eyelid epidermis (Fig. 4). A comparable distribution pattern has been shown for human abdominal skin keratinocytes from healthy donors.[15] This ultrastructural result contributes to the functional meaning of HRNR during the final stages of terminal differentiation of keratinocytes and transformation into corneocytes.[15,25] Moreover, our iTEM results showed that immunogold-labeled HRNR antibodies are associated with amyloid-like nanostructures in eyelid keratinocytes and (para) keratinized epithelial cells of the meibomian gland excretory duct (Fig. 4). These nanostructures are formed from large multi-domain oligomers of so-called "intrinsically disordered proteins (IDP)," such as HRNR.[26] An ultrastructural localization study of another IDP, the glycine-rich protein (GRP)-1.8, showed similar results in protoxylem cells of French beans.[27,28] Interestingly, GRP may be involved in plant defense by various mechanisms.[29,30] Recent studies indicate the importance of the molecular self-assembly and formation of nanostructures on the antibacterial properties of several amphiphilic peptides.[31–33] Therefore, it is tempting to speculate that amyloid-like nanostructures of the IDP HRNR are part of the antimicrobial defense at epithelial barrier in humans, too. Our ultrastructural results may help to explain antimicrobial activity of HRNR in healthy skin. Here, the full-length 284 kDa HRNR precursor protein is processed by

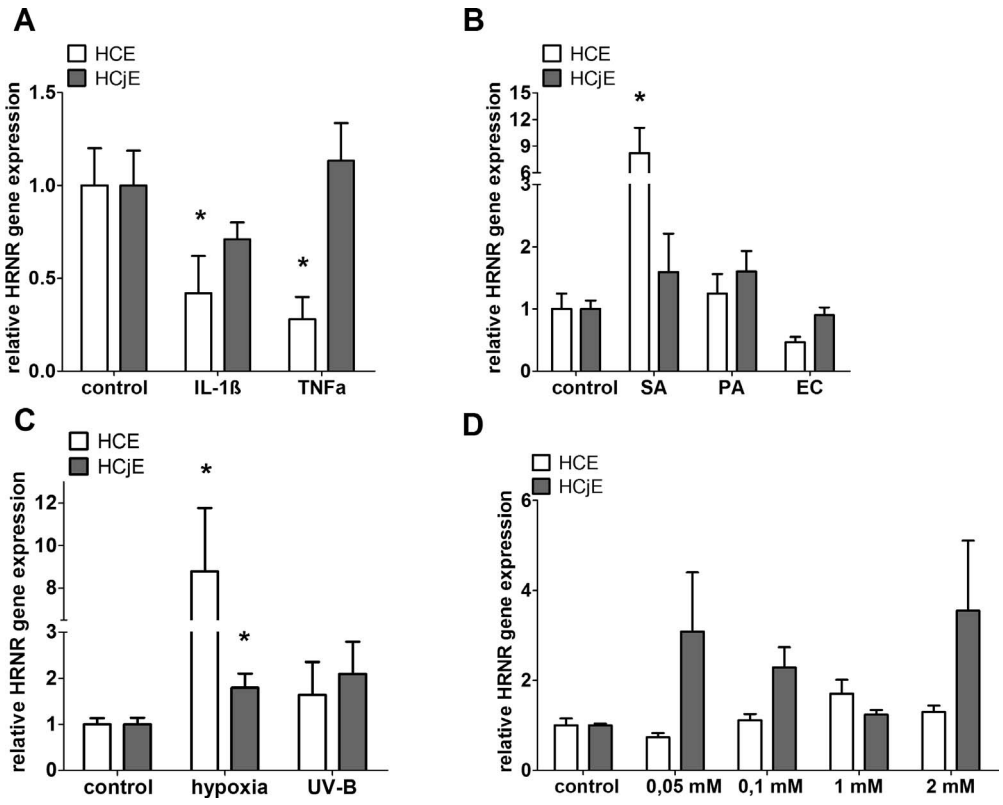

FIGURE 5. Regulation of *HRNR* gene expression in HCE and HCjE by means of real-time RT-PCR. Values are compared between stimulated and nonstimulated cells (control) after 24 hours. (**A**) Application of IL-1β or TNF-α (both 10 ng/mL) decrease *HRNR* gene expression in HCE but not in HCjE cells. (**B**) Supernatants of *S. aureus* (SA) induce *HRNR* gene expression in HCE cells, whereas supernatants of *P. aeruginosa* (PA) and *E. coli* (EC) show no significant effect. (**C**) Hypoxia increases *HRNR* gene expression in both cell lines. UV-B exposure has no effect on *HRNR* gene expression. (**D**) The *HRNR* gene expression is not affected by cultivation with elevated Ca^{2+} (0.05–2 mM). *Scale bars*: mean ± SEM of four up to eight independent experiments. Statistical significance is indicated by asterisks (1-way ANOVA, post hoc test; $^*P < 0.05$).

unknown mechanisms into multiple novel antimicrobial fragments, which show activity against gram-negative bacteria and fungi.[8,14] We also identified smaller HRNR fragments in tears of healthy donors (Fig. 1B). The proteases involved in this processing and its regulation at the ocular surface are unknown. Hypothetically, they proceed from internal proteases or bacterial proteases. In human epidermis, it has been shown that deimination of HRNR enhances cleavage by Calpain-1 protease and cross-linking by transglutaminases.[34] These results may indicate that HRNR not only could function as cytokeratin filament-associated structural protein, but also may contribute to limiting bacterial infection as a component of the innate defense system of the ocular surface barrier.

However, the evidence of the keratinization marker HRNR throughout the main duct epithelium of the meibomian gland is an indication of the keratinization potential of the whole duct system of meibomian gland. In healthy meibomian glands, only the terminal part of the excretory duct that opens to the posterior part of the lid margin normally shows keratinization.[35–37] Hyperkeratinization of the whole excretory duct epithelium is associated with obstruction of the orifice as well as changes in meibum composition with an increase in meibum viscosity.[38] Over time, this leads to glandular atrophy and finally to gland dropout and is termed meibomian gland dysfunction (MGD).[35] MGD leads to evaporative DED and is thought the leading cause of DED throughout the world.[39] Microarray analysis has demonstrated upregulation of genes for small proline-rich proteins (SPRR), Ca^{2+}-binding S100 proteins and cornulin in the meibomian glands of MGD patients compared to healthy controls.[40] Together with *HRNR* and *FLG2*, these genes are located on the EDC and also are associated with keratinization; epidermal cell differentiation and the cornified envelope.[10,41,42] In a previous study, we have shown functional expression of the *E. coli*-killing antimicrobial peptide psoriasin (S100A7)[43] in the lacrimal apparatus as well as in tears.[6] HRNR demonstrates a similar expression pattern especially with regard to the meibomian glands. However, currently it is not clear whether the (over)expression of EDC-associated proteins leads to MGD or whether maybe also is the primary cause of MGD. This must be addressed in further studies.

Furthermore, we analyzed regulation of HRNE gene expression by different stimuli to mimic inflammatory conditions as well as conditions associated with ocular surface stress. Our real-time RT-PCR results show induction of *HRNR* gene expression in HCE cells after treatment with supernatant of *S. aureus*, whereas supernatants of *P. aeruginosa* or *E. coli* did not reveal any HRNR induction in HCE as well as HCjE cells (Fig. 5B). Infection with *Staphylococcus* species is the major cause of bacterial conjunctivitis in adults.[44] Interestingly, the proinflammatory cytokines IL-1β and TNF-α significantly reduced *HRNR* gene expression in HCE but demonstrated no effect in HCjE cells (Fig. 5A). Usually, both cytokines induce expression of AMPs in both cell lines and also at the ocular surface.[2] In contrast, Abedin et al.[45] showed decreased gene expression of AMP human beta-defensin 9 in case of DED as well as in various patients with ocular surface infection. Further results revealed induction of *HRNR* gene expression after cultivation of HCE as well as HCjE cells under hypoxic conditions (Fig. 5C) to simulate decreased oxygenation of the

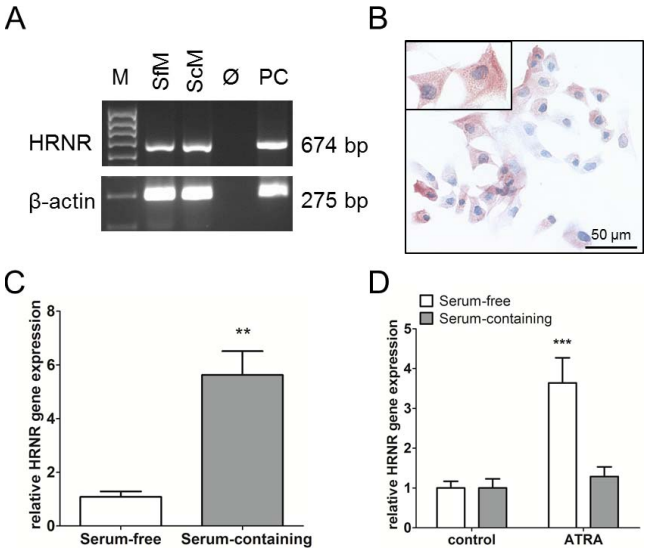

FIGURE 6. *HRNR* gene expression and regulation in the human meibomian gland epithelial cell line HMGEC. (**A**) RT-PCR results show *HRNR* gene expression in HMGECs cultivated in SfM as well as in ScM. Controls without *RT* step in cDNA synthesis (ø) and with cDNA from human skin (PC) were used. (**B**) Immunoreactivity of HRNR antibodies (*red*) in serum-differentiated HMGECs. (**C**). Real-time RT-PCR analysis shows induction of *HRNR* gene expression in serum-induced HMGECs compared to serum-free cultivated HMGECs. (**D**) ATRA (2 µM) induces *HRNR* gene expression in serum-free cultivated HMGECs but not in HMGECs cultivated in ScM. *Scale bars*: mean ± SEM of four up to eight independent experiments. Statistical significance is indicated by asterisks (1-way ANOVA, post hoc test; $^{**}P < 0.01$, $^{***}P < 0.001$).

ocular surface during contact lens wear.[46,47] Contact lens wear is associated with DED and is thought to be the major reason for contact lens intolerance based on mechanical stress through contact lenses and irritation of the lid margin.[48] In the context with our present HRNR results, it would be conceivable that hypoxic conditions also led to an increase in the expression of EDC-associated proteins that trigger keratinization of meibomian gland excretory ducts. Exposure to UV-B radiation as well as cultivation of HCE and HCjE with enhanced Ca^{2+} concentration, a trigger factor for keratinocyte differentiation, shows no effect on the *HRNR* gene expression in both analyzed cell lines (Fig. 5D). However, cell type-specific differences may explain the different results in ocular surface epithelial cells compared to keratinocytes. At the moment, trigger factors as well as regulatory mechanisms and signaling pathways for HRNR and other SFTPs at the ocular surface are unknown and need further elucidation.

As mention previously, we localized HRNE in human meibomian glands as well as in the immortalized HMGEC line. Gene expression analyses in HMGEC reveal a significant induction of *HRNR* gene expression after serum-induced differentiation and treatment with 2 µM ATRA (Fig. 6). Interestingly, ATRA had no effect on the *HRNR* gene expression in HMGECs cultivated in serum-containing medium. Various studies have shown that ATRA and other retinoic acid derivates have a negative effect on meibomian glands and promote MGD (see review[35]). In various animal models 13-cis retinoic acid (isotretinoin) is transformed to ATRA inside the body and induces keratinization in meibomian gland excretory ducts[49,50] In HMGECs, exposure to 13-cis retinoic acid inhibits cell proliferation induces apoptosis and alters gene expression.[51] In particular, certain genes of small proline-rich proteins, members of the EDC complex, are up-regulated by 13-cis retinoic acid.[51] In a previous study with HMGECs, we demonstrated induction of *HRNR* gene expression and other keratinization genes by MGD-associated sex hormones and increased calcium concentration.[23] However, HRNR would be a potential marker for the keratinization process leading to MGD-related DED. Further in vivo studies are needed to confirm HRNR expression and regulation in different MGD stages to analyze (hyper)keratinization processes in detail.

Our results suggested that FLG2 is not expressed and functionally active at the ocular surface and in the lacrimal apparatus of human. In an earlier study, FLG2 was examined in care solution extractions of silicone hydrogel contact lenses by liquid chromatography tandem mass spectrometry (Nano-LC-MS/MS).[52] Maybe samples were contaminated with corneocytes of lid epidermis leading to a FLG2 signal. Our immunohistochemistry results with anti FLG2 antibodies verified FLG2 expression in human epidermis,[9] including eyelids (Supplementary Fig. S1). Recent findings demonstrate that FLG2 is involved in the epidermal barrier function, accurate cornification in men and mice, and part of the natural moisturizing factor of the stratum corneum.[9,53,54] Moreover, skin-derived C-terminal FLG2 fragments show potent antimicrobial activity against *P. aeruginosa* and other *Pseudomonas* species by targeting bacterial replication.[16] At the ocular surface, a lubrication function through FLG2 is not necessary. Here, the tear film cleans and lubricates the ocular surface. However, it has been shown in the skin of burn patients that an absence of FLG2 is related to a higher susceptibility to *Pseudomonas* infection.[55] The total absence of FLG2 (fragments) at the ocular surface would be a possible explanation for the occurrence of *P. aeruginosa* infection. Beside *S. epidermidis*, gram-negative *P. aeruginosa* is the second most common pathogen leading to bacterial keratitis especially in association with contact lens wear.[56,57]

In summary, we demonstrated the expression and localization of HNRN at the ocular surface and in the lacrimal apparatus, as well as changes in the HNRN expression during various stress events in HCE but not HCjE cells. In contrast, FLG2 is not expressed and probably has no functional activity at the ocular surface and in the lacrimal apparatus. Our results suggested that HRNR is a component of the lacrimal apparatus and may contribute to maintaining the epithelial barrier at the ocular surface. Furthermore, HRNR seems to be involved in MGD, which must be confirmed in further studies.

Acknowledgments

The authors thank Maike Hemmerlein and Hong Nguyen for excellent technical assistance as well as Sylvia Dyczek for English proofreading. We acknowledge support by Deutsche Forschungsgemeinschaft and Friedrich-Alexander-Universität Erlangen-Nürnberg (FAU) within the funding program Open Access Publishing.

Supported by the Deutsche Forschungsgemeinschaft (DFG)–program grants PA 738/9-1 and PA 738/9-2, BMBF–Wilhelm Roux Program, Halle, Germany–program grants FKZ 09/16, 14/25, and 16/35, as well as Sicca Forschungsförderung of the professional Association of German Ophthalmologists. F.G. was supported by travel grant from European Federation for Experimental Morphology (EFEM) in 2017.

Disclosure: **F. Garreis**, None; **J. Jahn**, None; **K. Wild**, None; **D.B. Abrar**, None; **M. Schicht**, None; **J.-M. Schröder**, None; **F. Paulsen**, None

References

1. Tiffany JM. The normal tear film. *Dev Ophthalmol*. 2008;41:1–20.

2. McDermott AM. Antimicrobial compounds in tears. *Exp Eye Res*. 2013;117:53–61.
3. Gallo RL, Hooper LV. Epithelial antimicrobial defense of the skin and intestine. *Nat Rev Immunol*. 2012;12:503–516.
4. Harder J, Schröder J-M, Gläser R. The skin surface as antimicrobial barrier: present concepts and future outlooks. *Exp Dermatol*. 2013;22:1–5.
5. Garreis F, Gottschalt M, Paulsen FP. Antimicrobial peptides as a major part of the innate immune defense at the ocular surface. *Dev Ophthalmol*. 2010;45:16–22.
6. Garreis F, Gottschalt M, Schlorf T, et al. Expression and regulation of antimicrobial peptide psoriasin (S100A7) at the ocular surface and in the lacrimal apparatus. *Invest Ophthalmol Vis Sci*. 2011;52:4914–4922.
7. Garreis F, Schlorf T, Worlitzsch D, et al. Roles of human beta-defensins in innate immune defense at the ocular surface: arming and alarming corneal and conjunctival epithelial cells. *Histochem Cell Biol*. 2010;134:59–73.
8. Wu Z, Meyer-Hoffert U, Reithmayer K, et al. Highly complex peptide aggregates of the S100 fused-type protein hornerin are present in human skin. *J Invest Dermatol*. 2009;129:1446–1458.
9. Wu Z, Hansmann B, Meyer-Hoffert U, Glaser R, Schroder JM. Molecular identification and expression analysis of filaggrin-2, a member of the S100 fused-type protein family. *PLoS One*. 2009;4:e5227.
10. Mischke D, Korge BP, Marenholz I, Volz A, Ziegler A. Genes encoding structural proteins of epidermal cornification and S100 calcium-binding proteins form a gene complex ("epidermal differentiation complex") on human chromosome 1q21. *J Invest Dermatol*. 1996;106:989–992.
11. Marenholz I, Volz A, Ziegler A, et al. Genetic analysis of the epidermal differentiation complex (EDC) on human chromosome 1q21: chromosomal orientation, new markers, and a 6-Mb YAC contig. *Genomics*. 1996;37:295–302.
12. Henry J, Toulza E, Hsu CY, et al. Update on the epidermal differentiation complex. *Front Biosci*. 2012;17:1517–1532.
13. Takaishi M, Makino T, Morohashi M, Huh NH. Identification of human hornerin and its expression in regenerating and psoriatic skin. *J Biol Chem*. 2005;280:4696–4703.
14. Wu ZH, Meyer-Hoffert U, Bartels J, He YH, Harder J, Schroeder JM. Antimicrobially active hornerin peptides as protective factors of healthy skin. *J Invest Dermatol*. 2007;127:S2.
15. Henry J, Hsu CY, Haftek M, et al. Hornerin is a component of the epidermal cornified cell envelopes. *FASEB J*. 2011;25:1567–1576.
16. Hansmann B, Schroder JM, Gerstel U. Skin-derived C-terminal filaggrin-2 fragments are pseudomonas aeruginosa-directed antimicrobials targeting bacterial replication. *PLoS Path*. 2015;11:e1005159.
17. Tong L, Lan WW, Lim RR, Chaurasia SS. S100A Proteins as molecular targets in the ocular surface inflammatory diseases. *Ocular Surf*. 2014;12:23–31.
18. Posa A, Bräuer L, Schicht M, Garreis F, Beileke S, Paulsen F. Schirmer strip vs. capillary tube method: non-invasive methods of obtaining proteins from tear fluid. *Ann Anat*. 2013;195:137–142.
19. Gipson IK, Spurr-Michaud S, Argueso P, Tisdale A, Ng TF, Russo CL. Mucin gene expression in immortalized human corneal-limbal and conjunctival epithelial cell lines. *Invest Ophthalmol Vis Sci*. 2003;44:2496–2506.
20. Araki-Sasaki K, Ohashi Y, Sasabe T, et al. An SV40-immortalized human corneal epithelial cell line and its characterization. *Invest Ophthalmol Vis Sci*. 1995;36:614–621.
21. Liu S, Hatton MP, Khandelwal P, Sullivan DA. Culture, immortalization, and characterization of human meibomian gland epithelial cells. *Invest Ophthalmol Vis Sci*. 2010;51:3993–4005.
22. Garreis F, Schröder A, Reinach PS, et al. Upregulation of transient receptor potential vanilloid type-1 channel activity and Ca2+ Influx dysfunction in human pterygial cells. *Invest Ophthalmol Vis Sci*. 2016;57:2564–2577.
23. Schröder A, Abrar DB, Hampel U, Schicht M, Paulsen F, Garreis F. In vitro effects of sex hormones in human meibomian gland epithelial cells. *Exp Eye Res*. 2016;151:190–202.
24. Samarawickrama C, Chew S, Watson S. Retinoic acid and the ocular surface. *Surv Ophthalmol*. 2015;60:183–195.
25. Candi E, Schmidt R, Melino G. The cornified envelope: a model of cell death in the skin. *Nat Rev Mol Cell Biol*. 2005;6:328–340.
26. Dyson HJ, Wright PE. Intrinsically unstructured proteins and their functions. *Nat Rev Mol Cell Biol*. 2005;6:197–208.
27. Ryser U, Keller B. Ultrastructural localization of a bean glycine-rich protein in unlignified primary walls of protoxylem cells. *Plant Cell*. 1992;4:773–783.
28. Ryser U, Schorderet M, Zhao GF, et al. Structural cell-wall proteins in protoxylem development: evidence for a repair process mediated by a glycine-rich protein. *Plant J*. 1997;12:97–111.
29. Ueki S, Citovsky V. The systemic movement of a tobamovirus is inhibited by a cadmium-ion-induced glycine-rich protein. *Nat Cell Biol*. 2002;4:478–485.
30. Fu ZQ, Guo M, Jeong BR, et al. A type III effector ADP-ribosylates RNA-binding proteins and quells plant immunity. *Nature*. 2007;447:284–288.
31. Chang R, Subramanian K, Wang M, Webster TJ. Enhanced antibacterial properties of self-assembling peptide amphiphiles functionalized with heparin-binding cardin-motifs. *ACS Appl Matr Interface*. 2017;9:22350–22360.
32. Zhang YY, Algburi A, Wang N, et al. Self-assembled cationic amphiphiles as antimicrobial peptides mimics: role of hydrophobicity, linkage type, and assembly state. *Nanomed-Nanotechnol*. 2017;13:343–352.
33. Chen CX, Pan F, Zhang SZ, et al. Antibacterial activities of short designer peptides: a link between propensity for nanostructuring and capacity for membrane destabilization. *Biomacromolecules*. 2010;11:402–411.
34. Hsu CY, Gasc G, Raymond AA, et al. Deimination of human hornerin enhances its processing by calpain-1 and its cross-linking by transglutaminases. *J Invest Dermatol*. 2017;137:422–429.
35. Knop E, Knop N, Millar T, Obata H, Sullivan DA. The international workshop on meibomian gland dysfunction: report of the subcommittee on anatomy, physiology, and pathophysiology of the meibomian gland. *Invest Ophthalmol Vis Sci*. 2011;52:1938–1978.
36. Jester JV, Nicolaides N, Smith RE. Meibomian gland studies: histologic and ultrastructural investigations. *Invest Ophthalmol Vis Sci*. 1981;20:537–547.
37. Tektas OY, Yadav A, Garreis F, et al. Characterization of the mucocutaneous junction of the human eyelid margin and meibomian glands with different biomarkers. *Ann Anat*. 2012;194:436–445.
38. Paulsen F, Garreis F. What drives Meibomian gland disease? [in Spanish]. *Arch Soc Esp Oftalmol*. 2014;89:175–176.
39. Nichols KK, Foulks GN, Bron AJ, et al. The International Workshop on Meibomian Gland Dysfunction: executive summary. *Invest Ophthalmol Vis Sci*. 2011;52:1922–1929.
40. Liu S, Richards SM, Lo K, Hatton M, Fay A, Sullivan DA. Changes in gene expression in human meibomian gland dysfunction. *Invest Ophthalmol Vis Sci*. 2011;52:2727–2740.
41. Kypriotou M, Huber M, Hohl D. The human epidermal differentiation complex: cornified envelope precursors, S100

Investigative Ophthalmology & Visual Science

proteins and the 'fused genes' family. *Exp Dermatol*. 2012;21:643–649.

42. Contzler R, Favre B, Huber M, Hohl D. Cornulin, a new member of the "fused gene" family, is expressed during epidermal differentiation. *J Invest Dermatol*. 2005;124:990–997.
43. Gläser R, Harder J, Lange H, Bartels J, Christophers E, Schröder JM. Antimicrobial psoriasin (S100A7) protects human skin from Escherichia coli infection. *Nat Immunol*. 2005;6:57–64.
44. Epling J. Bacterial conjunctivitis. *BMJ Clin Evid*. 2012;2012:0704.
45. Abedin A, Mohammed I, Hopkinson A, Dua HS. A novel antimicrobial peptide on the ocular surface shows decreased expression in inflammation and infection. *Invest Ophthalmol Vis Sci*. 2008;49:28–33.
46. McMahon TT, Zadnik K. Twenty-five years of contact lenses: the impact on the cornea and ophthalmic practice. *Cornea*. 2000;19:730–740.
47. Natsumeda NH, Fatt I. Corneal swelling and oxygen flux through a soft contact lens. *Am J Optom Physiol Optics*. 1981;58:590–593.
48. Nichols JJ, Ziegler C, Mitchell GL, Nichols KK. Self-reported dry eye disease across refractive modalities. *Invest Ophthalmol Vis Sci*. 2005;46:1911–1914.
49. Lambert RW, Smith RE. Effects of 13-cis-retinoic acid on the hamster meibomian gland. *J Invest Dermatol*. 1989;92:321–325.
50. Lambert R, Smith RE. Hyperkeratinization in a rabbit model of meibomian gland dysfunction. *Am J Ophthalmol*. 1988;105:703–705.
51. Ding J, Kam WR, Dieckow J, Sullivan DA. The influence of 13-cis retinoic acid on human meibomian gland epithelial cells. *Invest Ophthalmol Vis Sci*. 2013;54:4341–4350.
52. Emch AJ, Nichols JJ. Proteins identified from care solution extractions of silicone hydrogels. *Optom Vis Sci*. 2009;86:E123–E131.
53. Hsu CY, Henry J, Raymond AA, et al. Deimination of human filaggrin-2 promotes its proteolysis by calpain 1. *J Biol Chem*. 2011;286:23222–23233.
54. Pendaries V, Le Lamer M, Cau L, et al. In a three-dimensional reconstructed human epidermis filaggrin-2 is essential for proper cornification. *Cell Death Dis*. 2015;6:e1656.
55. Branski LK, Al-Mousawi A, Rivero H, Jeschke MG, Sanford AP, Herndon DN. Emerging infections in burns. *Surg Infect*. 2009;10:389–397.
56. Bourcier T, Thomas F, Borderie V, Chaumeil C, Laroche L. Bacterial keratitis: predisposing factors, clinical and microbiological review of 300 cases. *Br J Ophthalmol*. 2003;87:834–838.
57. Wang N, Yang Q, Tan Y, Lin L, Huang Q, Wu K. Bacterial spectrum and antibiotic resistance patterns of ocular infection: differences between external and intraocular diseases. *J Ophthalmol*. 2015;2015:813979.

Investigative Ophthalmology & Visual Science